

Strongly Anisotropic Orientational Relaxation of Water Molecules in Narrow Carbon Nanotubes and Nanorings

Biswaroop Mukherjee,^{†,§,*} Prabal K. Maiti,^{†,*} Chandan Dasgupta,^{†,§,*} and Ajay K. Sood^{†,*}

[†]Centre for Condensed Matter Theory, Department of Physics, Indian Institute of Science, Bangalore 560 012, India, [‡]Department of Physics, Indian Institute of Science, Bangalore 560 012, India, and [§]Condensed Matter Theory Unit, Jawaharlal Nehru Centre for Advanced Scientific Research, Bangalore 560 064, India

Confinement leads to dramatic changes in the structure and dynamics of water.¹ At the structural level, confinement may lead to new types of molecular order that are not present in the bulk. Confinement of water molecules in a space of a few molecular diameters in extent, such as narrow carbon nanotubes, leads to solidlike ordering^{2–5} even at room temperature. Water near surfaces also tends to order in layers, as has been probed by X-ray diffraction.⁶ Several experimental and simulation studies have demonstrated that the dynamic behavior of confined water molecules is markedly different from that of water molecules in the bulk. As seen in a variety of systems such as reverse micelles,^{7–11} water–lipid bilayers,¹² major and minor grooves of DNA,^{13–15} and surfaces of proteins,¹⁶ the dynamics of water molecules is severely affected by confinement or by the presence of interfaces. This generally results in a slowing down of the dynamics of both translational and orientational degrees of freedom. This general behavior is also true for the orientational dynamics of fluids like carbon disulfide¹⁷ and methyl iodide,¹⁸ confined inside nanoporous glasses, which have been studied by using optical Kerr effect (OKE) spectroscopy. An ideal system to study such confinement effects is water inside nanotubes and nanorings. Recent molecular dynamics (MD) simulations have revealed that water molecules spontaneously fill narrow hydrophobic cavities such as carbon nanotubes^{2–4,19–24}. The nanotube remains completely filled with water molecules throughout the duration of the simulations, the molecules exhibiting strongly correlated

ABSTRACT Molecular dynamics simulations of the orientational dynamics of water molecules confined in narrow carbon nanotubes and nanorings reveal that confinement leads to strong anisotropy in the orientational relaxation. The relaxation of the aligned dipole moments, occurring on a time scale of nanoseconds, is 3 orders of magnitude slower than that of bulk water. In contrast, the relaxation of the vector joining the two hydrogens is ten times faster compared to bulk, with a time scale of about 150 fs. The slow dipolar relaxation is mediated by the hopping of orientational defects, which are nucleated by the water molecules outside the tube, across the linear water chain.

KEYWORDS: carbon nanotubes · nanorings · water · confinement · hydrogen bonding defects · reorientational relaxation

motion along the axis of the tube. The chain of water molecules remains intact because the energy¹⁹ (7 kCal/mol $\sim 10k_B T$) of a hydrogen bond between neighboring water molecules is much larger than the thermal energy.

In this work, we use MD simulations to study the reorientational dynamics of water molecules inside narrow (6,6) carbon nanotubes and nanorings. In the nanotube simulations, open-ended nanotubes of several different lengths are held fixed in a bath of water. Water molecules confined in isolated, closed carbon nanorings are also studied in order to eliminate and understand the effects of the exchange of water molecules inside open-ended nanotubes with those in the bulk. The diameter of the tube/ring used in the simulations is 8 Å, which allows only a single file of water molecules inside the tube/ring. In our previous work,⁴ concerning the nature of diffusion of water molecules inside open-ended nanotubes, we have shown that the water molecules diffuse slowly inside the nanotube, the diffusion coefficients being roughly half of that of bulk water. In this work we dem-

*Address correspondence to biswa@physics.iisc.ernet.in, maiti@physics.iisc.ernet.in, cdgupta@physics.iisc.ernet.in, asood@physics.iisc.ernet.in.

Received for review March 24, 2008 and accepted May 20, 2008.

Published online June 07, 2008
10.1021/nn800182v CCC: \$40.75

© XXXX American Chemical Society

onstrate that the same confinement leads to a very strong anisotropy in the reorientational dynamics, manifested in a dramatic enhancement of the dynamics of some orientational degrees of freedom, while the dynamics of other orientational degrees of freedom are slowed down due to confinement. In particular, the orientational relaxation time of the average dipole moment of a water molecule inside the nanotube is found to be about 3 orders of magnitude longer than that of a water molecule in the bulk. It is observed that this relaxation occurs due to the diffusion of hydrogen bonding defects across the single file water chain. This relaxation time increases with the length of the nanotube because our calculations show that the local electric field at a point on the axis of the tube and just outside it grows with the length of the tube. We believe that the operative mechanism for the nucleation of these defects requires a water molecule just outside the tube to be oriented in a direction opposite to the local electric field at that point and this possibility becomes rarer as the length of the nanotube increases. In contrast, the time scale of relaxation of the vector that joins the two hydrogens in a molecule inside the nanotube is about ten times faster than the corresponding time scale for bulk water. This is the first study which points out that strong confinement can lead to a faster relaxation due to rearrangement of hydrogen bond network. The same reorientational behavior is also found in our simulations of water molecules inside isolated, closed carbon nanorings. The anisotropy in the reorientational dynamics of water molecules in nanorings is stronger than that of water molecules in open-ended nanotubes because interactions with the bulk through the open ends of a nanotube are not present in nanorings. The speeding up of the orientational relaxation of the vector that joins the two hydrogens in a confined molecule leads to a strong enhancement of the average rotational diffusion constant (as discussed below, the interpretation of the values of this diffusion constant needs some care). This dramatic effect of confinement is contrary to conventional wisdom according to which strong confinement should produce a slowing down of the dynamics.

The rest of the paper is arranged in the following way. In the next section we describe in detail our results for the reorientational dynamics of the confined water molecules followed by a section where we conclude and a final section which gives the details of the simulations.

RESULTS AND DISCUSSION

Reorientational Dynamics of Confined Water. The water molecules are tightly packed inside a nanotube due to hydrogen bonding, with the average density almost four times that of bulk water.¹⁹ The dipole moments of all the confined water molecules are almost always

aligned, pointing either “up” (along +z direction, see Figure 1a) or “down” (along -z direction). Their orientation changes by cooperative “flips” that take them from one of these state to the other. Inside the nanoring the water molecules tend to form clusters as shown in Figure 1b. The number of clusters depends on the average density of water molecules inside the nanoring. At a low filling fraction of 0.054, there is a single unipolar cluster. The water molecules within the cluster are all strongly hydrogen bonded with their dipole moments aligned. Simulations at intermediate filling fractions (between 0.1 and 0.5), starting from an initial state in which the water molecules are uniformly spaced inside the nanoring, show the formation of a long-lived state with two oppositely polarized clusters which repel each other because of electrostatic forces and therefore tend to stay at diametrically opposite sides in the ring (see Figure 1b). The lifetime of this two-cluster state depends on the filling fraction. For example, for a filling fraction of 0.43, this state exists for about 80 ns. After this time, the water molecules gradually break off from the smaller cluster and join the larger one, forming a single polarized cluster after 90 ns. Simulations for another 50 ns after this time show that the single cluster does not break up. At very high filling fractions of 0.9 and above, a single unipolar cluster is formed. Figure 2 shows the time-dependence of the axial component of the average dipole moment $M_z(t)$ of the confined water molecules, defined by

$$M_z(t) = \frac{1}{N(t)} \sum_{i=1}^{N(t)} \mathbf{p}_i(t) \cdot \mathbf{n} \quad (1)$$

where $\mathbf{p}_i(t)$ is unit vector along the dipole moment of the i th water molecule at time t , \mathbf{n} is the unit vector in the z-direction along the axis of the tube, and $N(t)$ is the number of water molecules inside the nanotube at time t . Figure 2 panels a and b show data for water confined inside 14 and 28 Å long nanotubes, respectively. The average number of confined water molecules is 5 and 10 inside the 14 and 28 Å nanotubes, respectively. The net dipole moment of the chain of water molecules makes collective flips between the “up” and “down” states. The mean time interval between successive flips increases with the length of the tube. The red curve in Figure 2b shows the time-dependence of the axial component of the average dipole moment of the water molecules in bulk water outside the nanotube. This clearly shows that confinement leads to ordering of the dipole moments of the water molecules. Figure 2c shows the axis projected net dipole moment of the water molecules inside the nanoring at a filling fraction of 0.054 (10 water molecules, single polarized cluster). The dipolar flips are much more infrequent in this case, as compared to the water molecules inside the 28 Å open-ended nanotube. This is because the bath of water mol-

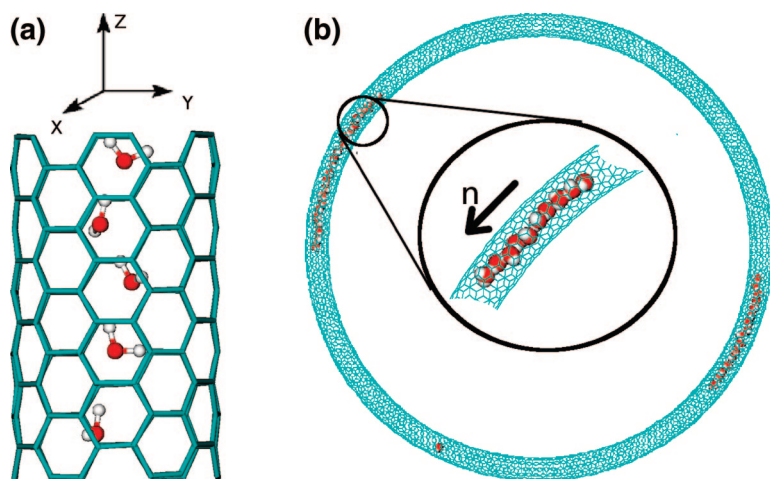


Figure 1. Snapshots of water molecules inside the 14 Å nanotube (a) and the nanoring at a filling fraction of 0.21 (40 molecules) (b). Both figures show the clustering of the water molecules due to strong hydrogen bonding. All the dipoles of the water molecules in a cluster are aligned. The coordinate axes mentioned in the text are also marked.

ecules outside the nanotube, which initiates the flips *via* interactions through the open ends of the nanotube, is absent in the case of the nanoring.

The polarization flips in the open tubes are mediated by the introduction of orientational defects in the water chain. The orientational defects are of two types, the D and L defects.^{25,26} These defect configurations leave the number of hydrogen bonds unchanged compared to the defect-free chain but they provide barriers to the conduction of protons through single file water clusters.²⁵ Earlier simulations of single file water chains inside gramicidin channels also exhibit similar orientational defects.²⁷ The D defects in such situations are stabilized by the presence of charges on the inner walls of the gramicidin channel, but in the present situation the defects are short-lived because the surface of the carbon nanotube is charge free. The D defect has dipoles of the neighboring water molecules pointing into the defect, whereas the L defect has the dipoles of the neighboring water molecules pointing away. The possible mechanisms by which the defect enters the single file water chain of our simulation are the following. If the polarization of the confined water molecules is positive (the end corresponding to the tip of the polarization vector is referred to as the positive extreme, while the end corresponding to its tail is referred to as the negative extreme) and the defect enters from the positive extreme of the nanotube then it should be a D defect. On the other hand, when the polarization is positive and the defect enters from the negative extreme of the nanotube, it should be a L defect. However, the analysis of our simulation data shows that all the orientational flips occurs *via* the mediation of D defects, which enter the tube from the end at which the confined water molecules donate hydrogen bonds

to the surrounding water molecules. This observation is in agreement with ref 28. A cartoon of a particular orientational defect configuration, observed in our simulations is shown in Figure 3a. This is a D defect, which has entered from the positive extreme of the nanotube, when the polarization of the confined water molecules was positive. The water molecule at the location of the defect has its dipole pointing perpendicular to the axis of the tube and the water molecules on its either side are oppositely polarized. These defects enter from one end and can either hop across the whole chain and exit from the other end or can exit

from the end through which they entered. Only when they are able to hop across the whole chain does the polarization of the chain flip. The mean time between successive nucleations of defects is quite long (\sim several nanoseconds) and depends on the length of the nanotube, whereas the time taken by the defect to diffuse across the water chain is quite short (\sim several pi-

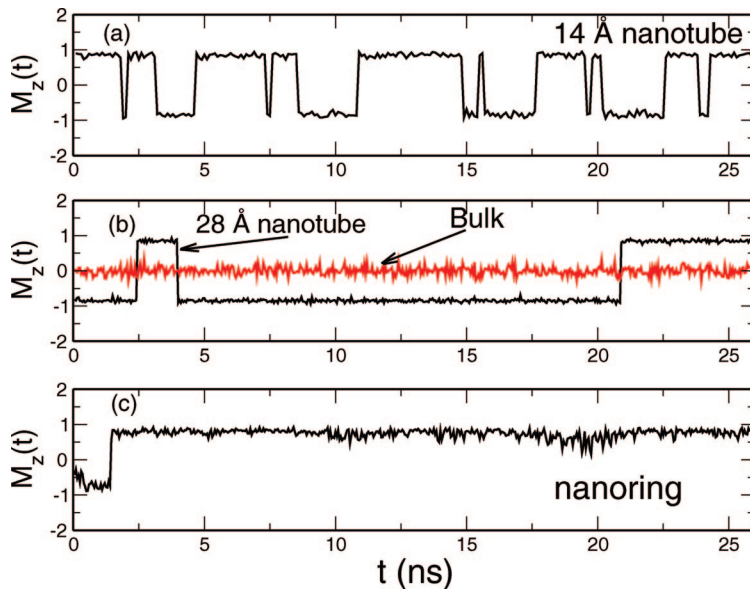


Figure 2. Panels a and b show the average dipole moment of the water molecules confined inside the 14 and 28 Å and nanotubes, respectively. The 14 and 28 Å tubes accommodate 5 and 10 water molecules on an average. The dipole moments of the water molecules inside the nanotube are mostly aligned in either “up” or “down” states, with cooperative flips between these two states. The flips become rarer as the length of the water chain increases. The red curve in panel b shows the axial component of the average dipole moment of the water molecules in the bulk, where there is no orientational order. Panel c shows the axial polarization of the system at a filling fraction of 0.054 (10 water molecules, single polarized cluster) inside the nanoring. Since the system of water molecules inside the nanoring is isolated the polarization flips are much rarer compared to the water molecules inside the open 28 Å tube, which accommodates 10 water molecules on the average.

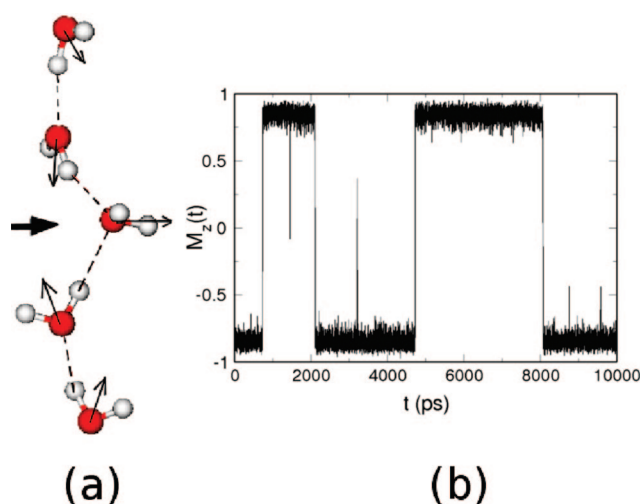


Figure 3. Panel a shows an orientational D defect in the water chain. The location of the defect is marked by an arrow. The transition between the “up” and “down” states in the open tube is mediated by the hopping of these orientational defects through the single file water chain, which are introduced in the water chain by the bulk water outside. These defects are introduced rarely, on a time scale (*ca.* several nanoseconds) which again depends on the length of the tube, but they diffuse through the water chain quickly (*ca.* several picoseconds). The dipole moments of the water molecules are marked by arrows and the hydrogen bonds between neighboring water molecules are marked by dashed lines. Panel b shows the $M_z(t)$ versus t for the water molecules inside the nanotube with 8 unit cells (18.6 Å) during an interval of 10 ns. Four successful and four unsuccessful attempts to flip the polarizations of the confined water chain take place during this interval.

coseconds). An approximate estimate of the speed at which the defects are nucleated into the polarized chain of the confined water molecules was done in the following way. We analyzed the $M_z(t)$ versus t data for a 100 ns long trajectory for two tube lengths, one with 8 unit cells (18.6 Å length) and the other with 18 unit cells (40.4 Å length). For both these data sets the number of successful and unsuccessful attempts to flip the net dipole moment were measured from the temporal variation of the average dipole moment, $M_z(t)$. Figure 3b shows the temporal variation of $M_z(t)$ for the water molecules confined inside a nanotube of length 18.6 Å during an interval of 10 ns. The criterion that we have used for characterizing an unsuccessful jump is the following: If the absolute value of $M_z(t)$ becomes less than 0.5 (this choice is ad hoc) and then $M_z(t)$ goes back to its initial extreme value of ± 0.85 we say that there has been an unsuccessful attempt to flip. For the nanotube with 8 unit cells (18.6 Å length) we record 61 unsuccessful and 31 successful flip attempts in a 100 ns long trajectory. For the nanotube with 18 unit cells (40.4 Å length) we record 28 unsuccessful and 9 successful attempts in the 100 ns long trajectory. These results show that it becomes progressively harder to introduce defects as one goes to longer tubes.

The length dependence of the time between nucleations of the defects can be understood from

a preliminary calculation of the local electric field owing to the confined water chain at a point on the axis of the nanotube, just outside it. The strength of this electric field increases with the length of the tube. For a defect to nucleate at the end of a nanotube, the water molecule in the immediate vicinity should have an orientation for which its dipole moment points in a direction opposite to the local electric field induced by the confined water molecules (the electric field induced by the outer water molecules is expected to cancel because of symmetry). This is energetically costly and the energy cost is $2pE$, where p is the dipole moment of a water molecule and E is the local electric field. By estimating the electric field due to the confined water molecules only, this energy cost is $\sim 4.6k_B T$ for the 14 Å tube and $\sim 10k_B T$ for the 56 Å tube. This provides a qualitative understanding of the observed increase in the mean time between successive defect nucleation with increasing tube length.

In addition to the temporal evolution of the average dipole moment, the ordering of the dipole moments of the confined water molecules is also evident from plots of the time-averaged distribution of the angle θ between the dipole moment and the axis of the tube. The axis is unique for the straight tube, whereas it depends on the location of the water molecule in the ring. In the case of the nanoring, the local axis has been defined as the tangent to the ring at the location of a water molecule (see Figure 1b). The inset of Figure 4 defines the angle θ . Figure 4 shows the distribution function $P(\theta)$ for the water molecules inside

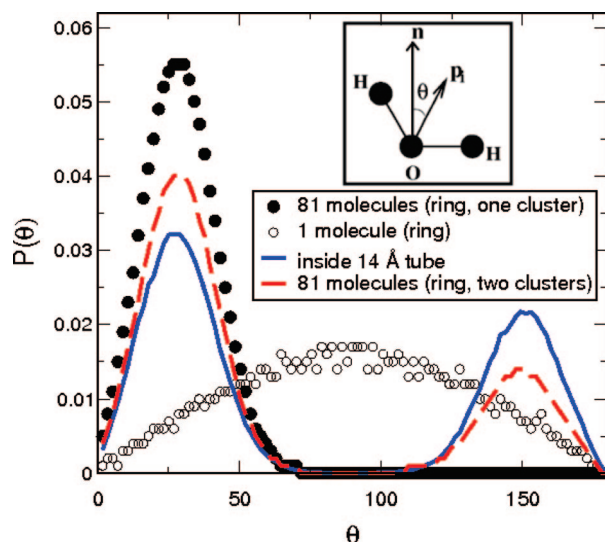


Figure 4. The time averaged distribution of the angle that the dipole moment of a water molecule makes with the local axis. Inset shows the angle θ , between the dipole moment vector p_i and the axis of the tube n . The distributions are shown for water molecules inside the nanoring at a filling fraction of 0.43, when there is a single polarized cluster (filled circles) and when there are two clusters (red, dashed line), for a single water molecule inside the nanoring (open circles) and for water molecules inside an open nanotube of length 14 Å, with averaging over a 50 ns trajectory (blue line).

the ring at a filling fraction of 0.43 when two oppositely polarized clusters are present (red, dashed line) and when the two clusters have merged into a single unipolar cluster (filled circles). On changing the initial conditions (the initial polarization), the details of which are given in Supporting Information, it is equally likely for this curve $P(\theta)$ to peak at an angle, which is a complement of its present peak angle. The distribution $P(\theta)$ for a single water molecule inside the nanoring is shown by open circles and $P(\theta)$ for water molecules inside the 14 Å open-ended tube is shown by the blue full line. It can be seen that the distribution function for the single molecule is much more isotropic than that for the molecules in the larger cluster, as the single molecule does not have any other water molecule with which to form hydrogen bonds. The distribution function for water molecules inside the 14 Å open-ended nanotube, obtained by averaging over a simulation time of 50 ns, is bimodal, with peak positions at 25° and 150°. These plots show that the dipole moment vectors are mostly either parallel or antiparallel to the local tangent vector at the location of the water molecule in the case of the nanoring and to the axis of the tube in the case of straight nanotubes. Similar $P(\theta)$ was also found for water molecules inside open carbon nanotubes.²⁹

Single particle reorientational motion of the water molecules can be analyzed by calculating the correlation function

$$C_l^\alpha(t) = \frac{\langle \sum_{i=1}^N P_l[\mathbf{e}_i^\alpha(t) \cdot \mathbf{e}_i^\alpha(0)] \rangle}{\langle \sum_{i=1}^N P_l[\mathbf{e}_i^\alpha(0) \cdot \mathbf{e}_i^\alpha(0)] \rangle} \quad (2)$$

where P_l is the Legendre polynomial of rank l and \mathbf{e}_i^α is one of unit vectors used to specify the orientation of the i th water molecule. Typically the vector \mathbf{e}^α is chosen to be along the line joining the hydrogen atoms, or along the net dipole moment of the water molecule or in a direction perpendicular to the HOH plane. In our calculations, we have taken \mathbf{e}^α either along the dipole moment of the water molecule or along the line joining the two hydrogens and we take the rank of the Legendre polynomial to be one ($l = 1$). At long times the functions $C_l^\alpha(t)$ decay exponentially. The inset in Figure 5a shows the orientational correlation function of the dipole moment of bulk TIP3P water molecules. The time scale of the long-time exponential decay of the dipolar orientational correlation functions is about 2.5 ps, which is close to values in ref 31. In contrast the dipolar orientational relaxation time-scale of the water molecules confined inside the nanotube or the nanoring is much longer. Figure 5a shows the orientational correlation of the dipole moment of water molecules confined inside the nanoring at a filling fraction of 0.43, after

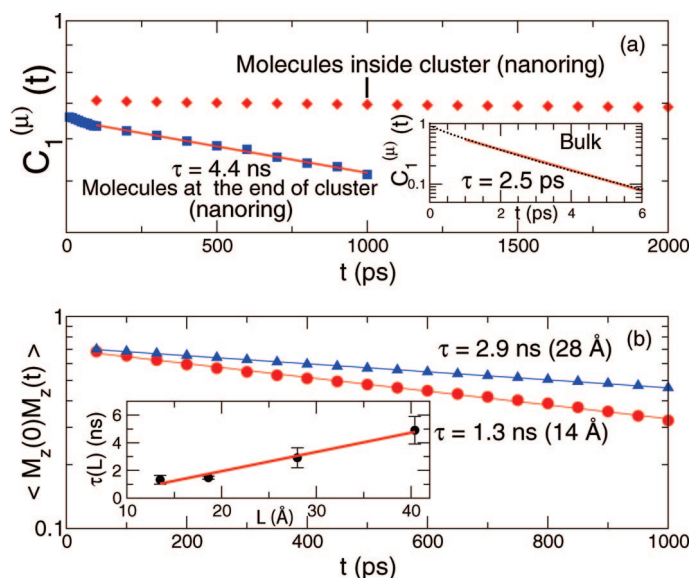


Figure 5. Panel a shows the reorientational correlation function of various groups of water molecules confined inside the ring, where the filling fraction is 0.43 and the molecules have formed a single unipolar cluster. The long-time decay of the orientational correlation function, which is supposed to be exponential is very slow for the water molecules within the cluster (denoted by diamond). The water molecules at the ends of the clusters (squares) relax faster than the central molecules. Bulk water molecules (inset) relax on time scales which are orders of magnitude faster. Panel b shows the time correlation function, $\langle M_z(0)M_z(t) \rangle$ for the confined water molecules inside the 14 Å (circles) and the 28 Å (triangles) tubes. The correlation functions have been fitted to an exponential yielding relaxation times of 1.3 and 2.9 ns for the 14 and the 28 Å nanotubes, respectively. The inset shows the scaling of the correlation time with the length of the nanotube.

the two clusters have merged to form a single unipolar giant cluster. The correlation function for the molecules within the cluster is shown by the diamond symbols, and the result for molecules at the ends of the cluster is shown by the square symbols. We see that for the water molecules in the middle of the cluster, the long-time relaxation of the reorientational correlations is very slow: in fact it does not decay at all within the time scale of the simulation. This is because each water molecule inside a cluster is hydrogen bonded to two of its nearest neighbors, constraining the orientational dynamics. The molecules at the ends of the clusters have less constraints and hence can relax faster compared to those inside the cluster. The water molecules at the end of the cluster have a relaxation time of 4.4 ns. For the water molecules inside the open nanotube, where there is a constant exchange of molecules with the outside bath, the analogous quantity to calculate is the time-correlation of the quantity $M_z(t)$ defined in eq 1. Figure 5b shows the time correlation function, $\langle M_z(0)M_z(t) \rangle$ (the angular brackets indicate an average over time-origins) for the confined water molecules inside the 14 Å (circles) and the 28 Å (triangles) tubes. The correlation functions have been fitted to an exponential decay, yielding relaxation times of 1.3 and 2.9 ns for the 14 and 28 Å nanotubes, respectively. Comparing Figure 5 panels a and b, it can be seen that the wa-

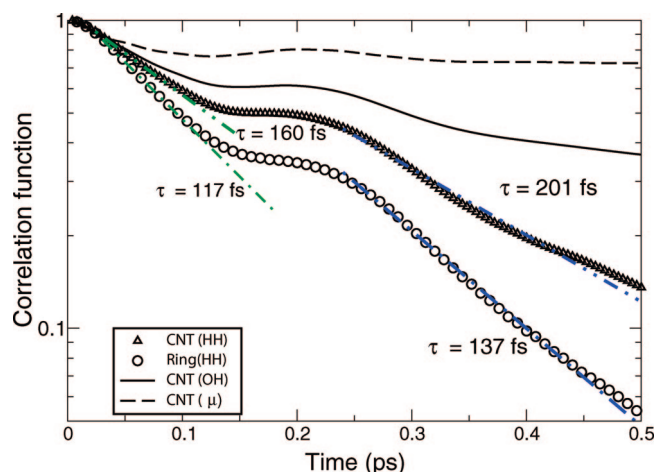


Figure 6. Anisotropy of the reorientational relaxation of dipole, **OH** and **HH** vectors. Such anisotropy is also present in bulk water, but is very mild. Under confinement in a cylindrical geometry it is dramatically magnified. The dipoles in the confined water (dashed line) relax extremely slowly on timescales of nanoseconds. The **HH** vectors of the molecules inside open nanotubes of length 56 Å (triangles) and inside rings (circles) (filling fraction is 0.43 and the molecules have formed a single unipolar cluster) relax very fast on timescales of a few hundreds of femtoseconds. The **OH** vector of the molecules inside the nanotube shows an intermediate behavior with relaxation time of about 30 ps.

ter molecules inside the nanoring relax more slowly compared to those inside the open nanotubes. This is because the constant interaction with the bath makes the reorientational relaxation of the dipoles of the water molecules inside the nanotubes faster compared to that inside the nanoring. For the water molecules in the open-ended nanotube, the relaxation time mentioned above is the average lifetime of the giant dipole in the “up” or “down” state. As discussed earlier, the details of the orientational rearrangements of the confined water molecules reveal that a flip between the “up” and “down” states occurs by the nucleation of a defect at one end of the chain, which then propagates through the chain to the other end to complete the flip. The inset of Figure 5b shows that the average lifetime in the “up” or “down” state scales linearly with the length of the nanotube, which is in agreement with ref 30.

We have also calculated the reorientational correlation function of the vector joining the two hydrogen atoms in a water molecule. This correlation function characterizes the rotational dynamics of a water molecule about its dipole moment vector. Interestingly, we observe that this rotational motion is dramatically enhanced as a result of confinement, both in open tubes and in nanorings. The reorientational correlation functions of the **HH** vector for the water molecules confined inside an open nanotube of 56 Å length (24 unit cells, 576 atoms) (triangles) and closed rings (circles) (filling fraction is 0.43 and the molecules have formed a single unipolar cluster) are shown in Figure 6. The short-time and long-time relaxation times are 117 and 137 fs for water inside the nanoring and 160 and 201 fs for open nanotubes. In bulk water it is known that the reorienta-

tional correlation function of the **HH** vector decays much more slowly with a time-constant of 2 ps.^{31,33} The fast **HH** relaxation of confined water is due to the fact that the hydrogen that does not participate in the hydrogen bonding with the next molecule in the chain is free to rotate without disrupting the hydrogen bond network, whereas in the bulk, each water molecule is tetrahedrally coordinated and hence has limited rotational freedom. In addition to the rotation of the water molecule about the dipolar axis, with one of the hydrogens participating in hydrogen bonding and the other free to rotate, there is yet another interesting mode in the motion of these hydrogen atoms. The bound hydrogen (*i.e.*, the one participating in the hydrogen bond with a neighboring water molecule) and the free hydrogen can exchange their positions. Such exchanges lead to large-amplitude angular jumps that are typically separated by a time interval of about 100 fs. Similar large jumps have been reported recently³² for water molecules in the bulk. Our observations demonstrate the occurrence of similar jump phenomena for confined water molecules also. These jump processes are responsible for the occurrence of the “plateau” near $t = 0.15$ ps in the plots in Figure 6. The details of these interesting microscopic processes and their manifestation in various temporal relaxations will be discussed in a separate paper.

The results described above show that cylindrically symmetric confinement causes the dipolar relaxation of a water molecule to slow down and the relaxation of the **HH** vector to speed up, thereby making the orientational relaxation strongly anisotropic. To demonstrate this anisotropy very clearly, we have plotted the orientational correlation functions of the dipole vector, the **OH** vector, and the **HH** vector of the confined water molecules in Figure 6. In bulk water the amount of this anisotropy is small and the relaxation times for all the three orientational correlation functions are very close to one another,^{31,33} with the dipole, **OH**, and **HH** vectors relaxing with timescales of 2.5, 2.3 and 2 ps, respectively (these relaxation plots are given in the Figure S1 of Supporting Information). The time scales of these relaxations change dramatically for the confined water with the dipole relaxing extremely slowly with a time scale of several nanoseconds, whereas the **HH** vector relaxes very fast with a time scale of about a few hundreds of femtoseconds. The relaxation of the **OH** vector orientation shows intermediate behavior with a relaxation time of about 30 ps. The large separation between the relaxation times of these three vectors illustrates a strong anisotropy in the orientational dynamics of the confined water molecules.

The fast rotation of the confined water molecules about the dipole axis is reflected in their average rotational diffusion constant. We have computed the rotational diffusion constant of water molecules from the time integral of the moment of inertia weighted angu-

lar velocity autocorrelation function.³⁴ The average rotational diffusion constant for the confined water is $D_R = 14.5 \times 10^{11} \text{ s}^{-1}$ and that of bulk TIP3P water is $D_R = 1.74 \times 10^{11} \text{ s}^{-1}$, (details in Supporting Information) showing an order of magnitude enhancement in the rotational diffusion constant for the strongly confined water molecules. The values of these diffusion constants should be interpreted with some caution: the reorientational relaxation of the confined water molecules is probably nondiffusive, as they involve large amplitude angular jumps. Hence, the result that the calculated average rotational diffusion constant of the confined water molecules is substantially larger than that in the bulk should be interpreted to convey only the information that the relaxation of certain rotational degrees of freedom (specifically, the rotational motion about the dipole moment vector) is much faster for the confined water molecules than that in the bulk.

CONCLUSION

In summary, our large-scale simulations of the orientational dynamics of water molecules inside open-ended narrow carbon nanotubes immersed in a bath of water and in isolated closed nanorings show that the confined water molecules form large chain-like clusters in which the dipole moments of the molecules are aligned. Orientational flips of this “giant” dipole occur at intervals of a few nanoseconds, which is very slow com-

pared to the dipolar relaxation time of bulk water (2.5 ps) and these flips occur by the diffusion of hydrogen bonding defects (D and L) across the water chain. The time between nucleation of these defects, just outside the nanotube, and the relaxation time of the average dipole moment of the confined water molecules grows as the length of the nanotube increases. The reorientational relaxation of the dipoles is even slower for the isolated water molecules inside the nanoring because the bulk water molecules, which initiated these flips in the water cluster confined inside the open-ended nanotubes, are not present in this case. Confinement also leads to a very strong anisotropy in the orientational relaxation. While the dipoles reorient very slowly, the reorientation of a confined water molecule about its dipole moment is much faster than that in the bulk. The effect of this accelerated rotation, is also manifested in an order of magnitude increase in the average rotational diffusion constant as compared to that for water molecules in the bulk. This is a rare example of confinement leading to an enhancement of orientational relaxation: most existing studies of the dynamics of water molecules in confined environments predict a slowing down of the dynamics (“immobilization”). We hope that our results will motivate new experimental investigations of the orientational dynamics of water molecules in narrow carbon nanotubes and perhaps also in nanorings.

SIMULATION DETAILS

Open-ended (6,6) carbon nanotubes of various lengths were placed in a bath of TIP3P³⁵ water molecules at 300 K and 1 atmosphere pressure. The simulations were performed using AMBER 7.³⁶ During the simulation the nanotubes were held fixed inside the simulation box, with its long axis along the z-direction (see Figure 1a). Simulations were performed for nanotubes of size 6 (144 atoms, 14 Å length), 8 (192 atoms, 18.6 Å), 12 (288 atoms, 28 Å), 18 (432 atoms, 40.4 Å) and 24 (576 atoms, 56 Å) unit cells. The simulation box contained about 1000 to 2200 water molecules depending on the size of the nanotube used. The interactions between various atoms were described by classical force fields; the carbon and oxygen atoms were modeled as Lennard-Jones particles with parameter values given in our earlier paper.⁴ The carbon–carbon bond length was 1.4 Å and the corresponding spring constant was 938 kcal/(mol Å²); the equilibrium C–C–C angle was $2\pi/3$ radians and the corresponding spring constant was 126 kcal/(mol rad²). The carbon nanoring, prepared by folding a (6,6) nanotube with 4880 carbon atoms (200 unit cells), was filled with TIP3P³⁵ water molecules at various filling fractions between 0.027 (5 water molecules) and 0.95 (179 water molecules). The radius of the nanoring is 78 Å. The nanotubes and nanorings were held fixed in a stiff harmonic external potential during the simulation. Fixing of the nanotubes is not necessary, it just makes the calculations simpler as one does not have to keep track of the motion of the nanotube in studying the dynamics of the confined water molecules.

The H–C dispersive interaction is neglected in the TIP3P model of water used in this work. In our view inclusion of such interactions will have negligible effects on our observations. The typical carbon–oxygen LJ energy scale is about $0.19 k_B T$ (T is taken as 300 K), whereas the carbon–hydrogen LJ energy scale is $0.07 k_B T$, which is less than half of the carbon–oxygen interaction. Further, these energy scales are much smaller than the hy-

drogen bond energy ($\sim 10 k_B T$), which is the key interaction responsible for all these interesting effects. The rest of the details of the simulations is given in Supporting Information.

Acknowledgment. B.M. would like to thank JNCASR for financial support and T. Cagin and N. Vidyasagar for helpful discussions. A.K.S. and P.K.M. thank the Department of Science & Technology, India, for financial support.

Supporting Information Available: Additional details of the simulation and details of the calculation of rotational diffusion constant; Figure S1 shows the reorientational relaxation of dipole, **OH**, and **HH** vectors in bulk water. This material is available free of charge via the Internet at <http://pubs.acs.org>.

REFERENCES AND NOTES

1. Zangi, R. Water Confined to a Slab Geometry: A Review Of Recent Computer Simulation Studies. *J. Phys.: Condens. Matter* **2004**, *16*, S5371–S5388.
2. Koga, K.; Parra, R. D.; Tanaka, H.; Zeng, X. C. Ice Nanotube: What Does the Unit Cell Look Like. *J. Chem. Phys.* **2000**, *113*, 5037–5041.
3. Koga, K.; Gao, G. T.; Tanaka, H.; Zeng, X. C. Formation of Ordered Ice Nanotubes inside Carbon Nanotubes. *Nature* **2001**, *412*, 802–805.
4. Mukherjee, B.; Maiti, P. K.; Dasgupta, C.; Sood, A. K. Strong Correlations and Fickian Water Diffusion in Narrow Carbon Nanotubes. *J. Chem. Phys.* **2007**, *126*, 1–8, 124704.
5. Mukherjee, B.; Maiti, P. K.; Dasgupta, C.; Sood, A. K. Structure and Dynamics of Confined Water Inside Narrow Carbon Nanotubes. *J. Nanosci. Nanotechnol.* **2007**, *7*, 1796–1799.
6. Toney, M. F.; Howard, J. N.; Richer, J. N.; Borges, G. L.; Gordon, J. G.; Melroy, O. R.; Wiesler, D. G.; Yee, D.;

- Sorensen, L. B. Voltage-dependent Ordering of Water Molecules at an Electrode-Electrolyte Interface. *Nature* **1994**, *368*, 444–446.
7. Faeder, J.; Ladanyi, B. M. Molecular Dynamics Simulations of the Interior of Aqueous Reverse Micelles. *J. Phys. Chem. B* **2000**, *104*, 1033–1046.
 8. Harpham, M.; Ladanyi, B. M.; Levinger, N. E. Water Motion in Reverse Micelles Studied by Quasielastic Neutron Scattering and Molecular Dynamics Simulations. *J. Chem. Phys.* **2004**, *121*, 7855–7868.
 9. Senapati, S.; Berkowitz, M. L. Water Structure and Dynamics in Phosphate Fluorosurfactant Based Reverse Micelle: A Computer Simulation Study. *J. Chem. Phys.* **2003**, *118*, 1937–1944.
 10. Dokter, A. M.; Woutersen, S.; Bakker, H. J. Inhomogeneous Dynamics in Confined Water Nanodroplets. *Proc. Natl. Acad. Sci. U.S.A.* **2006**, *103*, 15355–15358.
 11. Balasubramanian, S.; Pal, S.; Bagchi, B. Hydrogen-Bond Dynamics Near a Micellar Surface: Origin of the Universal Slow Relaxation at Complex Aqueous Interfaces. *Phys. Rev. Lett.* **2002**, *89*, 115505–1–115505–4.
 12. Bhide, S. Y.; Berkowitz, M. L. The Behavior of Reorientational Correlation Functions of Water at the Water-Lipid Bilayer Interface. *J. Chem. Phys.* **2006**, *125*, 094713–1–094713–7.
 13. Bagchi, B. Water Dynamics in the Hydration Layer Around Proteins and Micelles. *Chem. Rev.* **2005**, *105*, 3198–3219.
 14. Pal, S.; Maiti, P. K.; Bagchi, B. Anisotropic and Sub-Diffusive Water Motion at the Surface of DNA and of an Anionic Micelle CsPFO. *J. Phys.: Condens. Matter* **2005**, *17*, S4317–S4331.
 15. Pal, S.; Maiti, P. K.; Bagchi, B.; Hynes, J. T. Multiple Time Scales in Solvation Dynamics of DNA in Aqueous Solution: The Role of Water, Counterions, and Cross-Correlations. *J. Phys. Chem. B* **2006**, *110*, 26396–26402.
 16. Pal, S. K.; Zewail, A. H. Dynamics of Water in Biological Recognition. *Chem. Rev.* **2004**, *104*, 2099–2123.
 17. Loughnane, B. J.; Scodinu, A.; Fourkas, J. T. Extremely Slow Dynamics of a Weakly Wetting Liquid at a Solid/Liquid Interface: CS₂ Confined in Nanoporous Glasses. *J. Phys. Chem. B* **1999**, *103*, 6061–6068.
 18. Loughnane, B. J.; Fourkas, J. T. Geometric Effects in the Dynamics of a Nonwetting Liquid in Microconfinement: An Optical Kerr Effect Study of Methyl Iodide in Nanoporous Glasses. *J. Phys. Chem. B* **1998**, *102*, 10288–10294.
 19. Hummer, G.; Rasaiah, J. C.; Noworyta, J. P. Water Conduction Through the Hydrophobic Channel of a Carbon Nanotube. *Nature* **2001**, *414*, 188–190.
 20. Beckstein, O.; Biggin, P. C.; Sansom, M. S. P. A Hydrophobic Gating Mechanism for Nanopores. *J. Phys. Chem. B* **2001**, *105*, 12902–12905.
 21. Beckstein, O.; Sansom, M. S. P. Liquid-Vapor Oscillations of Water in Hydrophobic Nanopores. *Proc. Natl. Acad. Sci. U.S.A.* **2003**, *100*, 7063–7068.
 22. Striolo, A.; Chialvo, A. A.; Gubbins, K. E.; Cummings, P. T. Water in Carbon Nanotubes: Adsorption Isotherms and Thermodynamic Properties from Molecular Simulation. *J. Chem. Phys.* **2005**, *122*, 234172–1–234172–14.
 23. Striolo, A. The Mechanism of Water Diffusion in Narrow Carbon Nanotubes. *Nano Lett.* **2006**, *6*, 633–639.
 24. Mashl, R. J.; Joseph, S.; Aluru, N. R.; Jakobsson, E. Anomalous Immobilized Water: A New Water Phase Induced by Confinement in Nanotubes. *Nano Lett.* **2003**, *3*, 589–592.
 25. Dellago, C.; Naor, M. M.; Hummer, G. Proton Transport through Water-Filled Carbon Nanotubes. *Phys. Rev. Lett.* **2003**, *90*, 105902–1–105902–4.
 26. Zimmerli, U.; Gonnet, P. G.; Walther, J. H.; Koumoutsakos, P. Curvature Induced L-Defects in Water Conduction in Carbon Nanotubes. *Nano Lett.* **2005**, *5*, 1017–1022.
 27. Pomes, R.; Roux, B. Molecular Mechanism of H⁺ Conduction in the Single-File Water Chain of the Gramicidin Channel. *Biophys. J.* **2002**, *82*, 2304–2316.
 28. Best, R. B.; Hummer, G. Reaction Coordinates and Rates from Transition Paths. *Proc. Natl. Acad. Sci. U.S.A.* **2005**, *102*, 6732–6737.
 29. Zhu, F.; Schulten, K. Electrostatic Tuning of Permeation and Selectivity in Aquaporin Water Channels. *Biophys. J.* **2003**, *85*, 236.
 30. Wan, R.; Lu, H.; Li, J.; Bao, J.; Hu, J.; Fang, H. Self-Induced Spontaneous Transport of Water Molecules Through a Symmetrical Nanochannel by Ratchetlike Mechanism. Available online via <http://arxiv.org/abs/physics/0607289v1>.
 31. Praprotnik, M.; Janezic, D. Molecular Dynamics Integration and Molecular Vibrational Theory. III. The Infrared Spectrum of Water. *J. Chem. Phys.* **2005**, *122*, 174103–1–174103–10.
 32. Laage, D.; Hynes, J. T. A Molecular Jump Mechanism of Water Reorientation. *Science* **2006**, *311*, 832–835.
 33. Spoel, D.; Maaren, P.; Berendsen, H. J. C. A Systematic Study of Water Models for Molecular Simulation: Derivation of Water Models Optimized for use With a Reaction Field. *J. Chem. Phys.* **1998**, *108*, 10220–10230.
 34. Lin, S. T.; Maiti, P. K.; Goddard III, W. A. Dynamics and Thermodynamics of Water in PAMAM Dendrimers at Subnanosecond Time Scales. *J. Phys. Chem. B* **2005**, *109*, 8663–8672.
 35. Jorgensen, W. L.; Chandrasekhar, J.; Madura, J. D.; Impey, R. W.; Klein, M. L. Comparison of Simple Potential Functions for Simulating Liquid Water. *J. Chem. Phys.* **1983**, *79*, 926–935.
 36. Case, D. A.; Pearlman, D. A.; Caldwell, J. W.; Cheatham T. E.; Wang, J.; Ross, W. S.; Simmerling, C.; Darden, T.; Merz, K. M.; Stanton, W. A.; *AMBER7. 7 Ed.*, University of California: San Francisco, CA, 1999.